

**DESIGN AND ANALYSIS OF AN AXIAL COMPRESSOR FOR A  
TURBOFAN ENGINE**

**Doğuş ÖZKAN<sup>1</sup>**  
**Kadir BÜYÜKHAMURKAR<sup>2</sup>**

<sup>1</sup>*National Defence University, Turkish Naval Academy, Mechanical  
Engineering, Istanbul, Turkey,*  
[dozkan@dho.edu.tr](mailto:dozkan@dho.edu.tr); ORCID: 0000-0002-3044-4310

<sup>2</sup>*Turkish Navy, Istanbul, Turkey,*  
[kbuyukhamurkar@gmail.com](mailto:kbuyukhamurkar@gmail.com); ORCID: 0000-0001-8902-4604

**Date of Receive: 04.03.2020**

**Date of Acceptance: 20.04.2020**

**ABSTRACT**

*Turbofan engines are used to provide thrust force by using the high temperature and pressure gases flow from the nozzle to move passenger planes or war jet planes. Turbofan engines consist of complicated parts such as axial fan, compressor, combustion chamber, turbine, which are manufactured with high engineering knowledge. Therefore, it needs to be well designed, analyzed and manufactured. In this study, an axial compressor of a warplane turbofan engine was designed and analyzed with AxStream software. Results were compared with real turbofan engine measured values, furthermore, computed fluid dynamic and strain analysis were performed to evaluate compressor design parameters. Results showed that the polyprotic efficiency of the designed compressor was 2 % higher than the actual compressor. Furthermore, similar pressure and temperature were obtained at the outlet of the designed compressor.*

**Keywords:** *Turbofan Engine, AxStream, Axial Compressor, Computed Fluid Dynamics.*

## TURBOFAN MOTOR İÇİN EKSENEL AKIŞLI KOMPRESÖR TASARIMI VE ANALİZİ

### ÖZ

*Turbofan motorları, yolcu uçaklarını veya savaş jet uçaklarını hareket ettirmek için nozülde gelen yüksek sıcaklık ve basınç gazlarını kullanarak itme kuvveti sağlamak için kullanılır. Turbofan motorları, yüksek mühendislik bilgisi ile üretilen aksel fan, kompresör, yanma odası, türbin gibi karmaşık parçalardan oluşur. Bu nedenle, iyi tasarlanmış, analiz edilmiş ve üretilmiş olmalıdır. Bu çalışmada, bir savaş uçağı turbofan motorunun aksel kompresörü AxStream yazılımı ile tasarlanmış ve analiz edilmiştir. Sonuçlar gerçek turbofan motor ölçüm değerleri ile karşılaştırılmış, ayrıca kompresör tasarım parametrelerini değerlendirmek için hesaplamalı akışkan dinamiği ve gerilme analizi yapılmıştır. Sonuçlar, tasarlanan kompresörün poliprotik verimliliğinin gerçek kompresörden % 2 daha yüksek olduğunu göstermiştir. Ayrıca, tasarlanan kompresörün çıkışında gerçek kompresör göre benzer basınç ve sıcaklık elde edilmiştir.*

**Anahtar Kelimeler:** Turbofan Motor, AxStream, Aksel Kompresör, Hesaplamalı Akışkan Dinamiği.

**NOMENCLATURE**

$Lu$  : Specific work coefficient

$U$  : Rotor speed

$Lu_z$  : Specific work gradient

$H$  : Head of the compressor

$h$  : Entalphy

$w$  : Relative velocity

$p$  : Pressure

$\gamma, \varphi$  : Stator/rotor velocity coefficient

$\dot{m}$  : Mass flow rate

$\rho$  : Density

$\bar{w}$  : Total pressure loss coefficient

$c$  : Absolute velocity

$A$  : Area

$s$  : Entrophy

$\bar{w}_N$  : Pressure loss coefficient of stator

$\bar{w}_R$  : Pressure loss coefficient of rotor

$p_2 = P(h_2, s_2)$  : Pressure function

$s_1 = S(p_1, h_1)$  : Entropy function

$\beta$  : Flow angle in relative frame

## **1. INTRODUCTION**

Turbojet engine has been started to use in aviation since 1941 by the invention of Franks Whittle [1]. The first turbojet engine consisted of a radial compressor, a single combustion chamber, turbine and it was a water-cooled engine [2]. Besides, turbo jet engines were modified and different kinds of engines have been manufactured such as turbo prop and turbofan that used in aviation [3]. Turbofan engines are the most commonly used aircraft propulsion both in civil and military aviation applications which has a large fan driven by turbine mechanical energy and a large amount of airflow through a duct around the engine [4]. The main parts of these engines axial fan, compressor, combustion chamber, turbine and nozzle [5]. Axial fan compresses the air which its pressure and temperature increase before entering the axial compressors [6]. Axial flow compressor increase, not only pressure but also the temperature of the air as a consequence of a given pressure ratio by changing the velocity and also enthalpy of the air [7, 8]. Axial compressors consist of stages in which one stage is formed by one stator and rotor blades [9]. Furthermore, compressor stage numbers can be up to 20 stages. The computer-aided design of an axial compressor has been the most common method with advance calculations. On the other hand, design can be analyzed by advanced techniques such as computed fluid dynamic (CFD) and strain analysis [10-12]. This study presents a novel approach to improve and compare an actual compressor performance that runs in warplanes by using advanced software. Therefore, AxStream software (manufactured by Softinway company) was used to design and analysis of 5 stages of an axial compressor by using compressor running parameters of a turbofan engine of a jet fighter in this study. Design and analysis results were compared to running parameters of this turbofan engine. Results showed that the design pressure of air at the exit of the compressors was % 93 similar to the real engine pressure value.

## **2. MATERIALS AND METHODS**

The main design parameters of the axial compressor for the turbofan engine can be seen in Table 1. The axial compressor was considered to consist of 5 stages and inlet temperature, the pressure was the out of the fan flow.

**Table 1.** Design parameters.

<b>Inputs</b>	<b>Units</b>	<b>Minimum</b>	<b>Maximum</b>
Inlet pressure	kPa	426.32	426.32
Inlet temperature	K	475	475
Total outlet pressure	kPa	2643.21	2643.21
Mass flow	kg/s	52.89	52.89
Inlet flow angle	tan.deg	90	90
Inlet guide vane outlet angle	tan.deg	70	70
Shaft rotation	rpm	22800	22800
Mean diameter	mm	450	600
1'st blade height	mm	50	80
Work coefficient ( $Lu/U_2^2$ )	-	0.1	0.5
Specific work gradient ( $Lu_z/Lu_{-1}$ )	-	0.1	0.5
Stage number	-	1	5
Hub diameter	mm	1.0	10000

The following fundamental energy, continuity and work equations were used to calculate the design outputs of the axial compressor, respectively [13]. Eq. 1 shows energy transfer per mass in an adiabatic flow that occurs in a rotating wheel with the angular speed of  $\omega$ .  $\dot{m}$  in Eq. 4 is the continuity downstream of the working wheel.

$$H = h + \frac{w^2 - U^2}{2} \quad (1)$$

$$s_0 = S\left(p, \frac{1}{\gamma^2} \left(h - (1 - \gamma^2)h_{0w}^*\right)\right) \quad (2)$$

$$s_0 = S\left(\frac{p_R^* - \bar{w}p_0}{1 - \bar{w}}, \quad h_R^* - \frac{U^2}{2} + \frac{U_0^2}{2}\right) \quad (3)$$

$$\dot{m} = \rho(p_2, h_2) \cdot w_2 \cdot \sin \beta_2 \cdot A_2 \quad (4)$$

$$H = h_1 + \frac{c_1^2}{2} - U_1 c_{1u} \quad (5)$$

$$p_1 = P\left(h_0^* - \frac{c_1^2}{2\varphi^2}, s_0^*\right) \quad (6)$$

$$h_1 = h_0^* - \frac{c_1^2}{2} \quad (7)$$

$$s_1 = S(p_1, h_1) \quad (8)$$

$$h_2 = H + \frac{c_2^2}{2} - \frac{W_2^2}{2} \quad (9)$$

$$s_2 = S\left(P\left(H + \frac{U_2^2}{2} - \bar{w}_w(p_{1R}^* - p_1)\right), s_1\right) \quad (10)$$

$$p_2 = P(h_2, s_2) \quad (11)$$

$$h_3 = h_2^* - \frac{c_3^2}{2} \quad (12)$$

$$s_3 = S(p_2^* - \overline{w}_N(p_2^* - p_2), h_2^*) \quad (13)$$

$$p_2 = P(h_2, s_2) \quad (14)$$

From the known velocity coefficients of  $\varphi$ ,  $\gamma$  or total pressure coefficient  $\overline{w}_w$ ,  $\overline{w}_N$  three equation that is shown in Eq. 15, 16 and 17 can be derived for the compressor stage.

$$k_2(\dot{m}, w_2) = 0 \quad (15)$$

$$k_3(\dot{m}, w_2, c_3) = 0 \quad (16)$$

$$k_0(\dot{m}, w_2, c_3) = 0 \quad (17)$$

AxStream software solves numerically by minimizing of  $k_2^2 + k_3^2 + k_0^2$  by a method of conjugated gradients. Here 2000 iteration was used to find the best solution to these equations with the residual target set to 3.0e-5 (=RMS). Results, such as efficiency, main dimensions, temperature, pressure, and power, were compared to real engine design and running parameters. Furthermore, 3D aerodynamic and stress calculations were performed to improve the design.

### **3. RESULT AND DISCUSSION**

#### **3.1. Main Design and Flow Results**

The optimum main dimensions of the designed 5 stages axial compressor is shown in Fig. 1(a) with % 87.9 total efficiency. The average compressor diameter was found to be 422.19 mm and the inlet guide vane height was 60.87 mm whereas the first stage rotor and stator blade height was found 48.49, 46.48 mm, respectively. The designed compressor 3D view was shown in Fig. 1(b). Furthermore, the enthalpy-entropy diagram in Fig. 1(c)

set out an enthalpy increase in the compressor which higher at the rotor blades than the stator blades. 1D and 2D streamline calculations are shown in Fig. 2, where inlet pressure was increased from 423 kPa to 2690 kPa and the total temperature at the exit increased to 835 K. Furthermore, inlet total enthalpy and total air velocity increased from 478 kJ/kg to 885 kJ/kg and 248.3 m/s to 457.9 m/s.

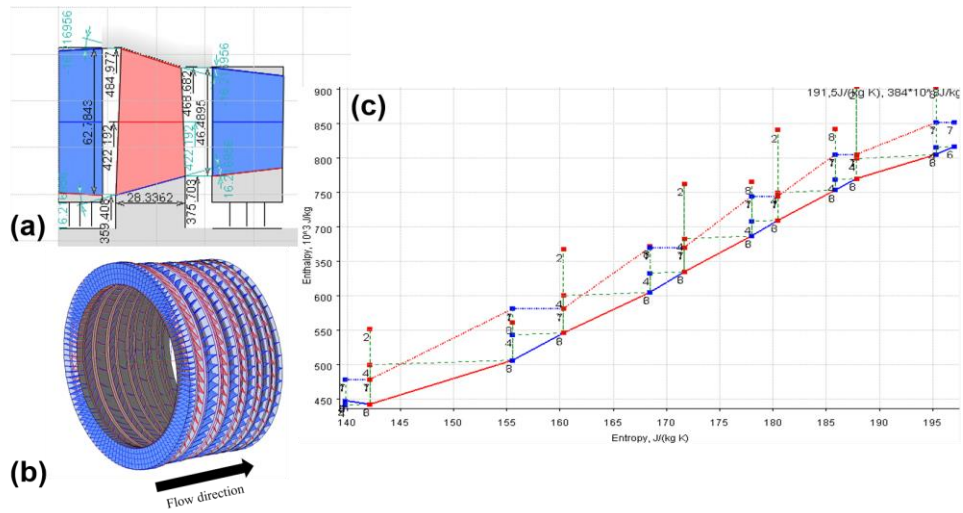


**Figure 1.** (a) 5 stages axial compressor with dimensions and inlet guide vanes (red blades are the rotor and blue ones are stator blades), (b) 3D image of the designed compressor, (c) enthalpy-entropy diagram of the designed compressor.

*Design and Analysis of an Axial Compressor for a Turbofan Engine*

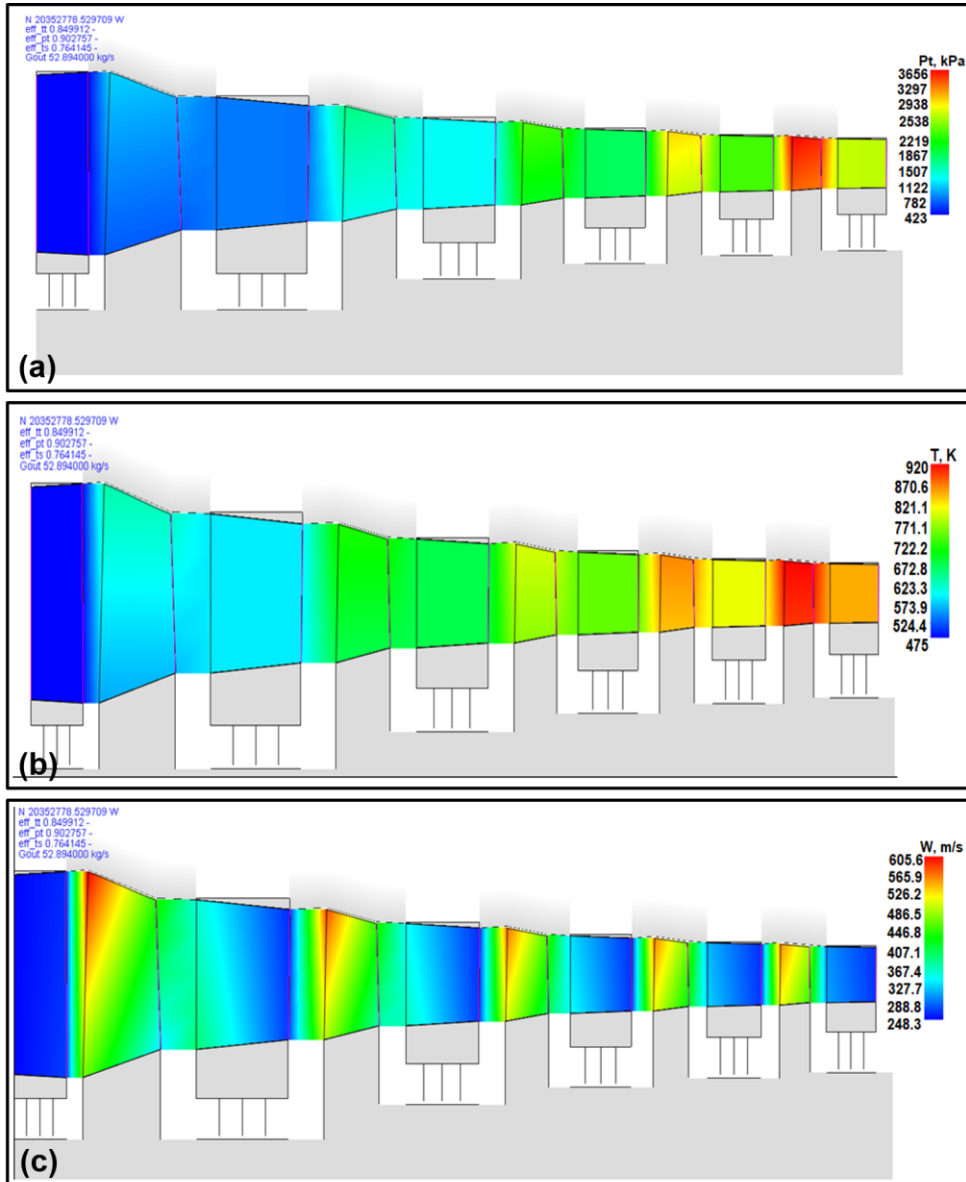


**Figure 2.** 1 and 2D flow calculations of axial compressor, (a) total pressure, (b) total temperature, (c) total velocity increase of the air at stages.

### **3.2. Stage Analysis of the Compressor**

In this section, detailed enthalpy, pressure, stress, velocity and computational fluid dynamic analysis (CFD) analysis of each stage of the axial compressor were evaluated. Vectorial velocity diagrams are shown with velocities and angles where  $A$  is the angle between angular and absolute velocity,  $B$  is the angle between angular and relative velocity,  $C$  is the absolute velocity,  $K1$ ,  $K2$  denotes inlet and outlet air angle of air according to the blade.

### 3.2.1. Inlet Guide Vanes (IGV)

The calculated absolute velocities and angles are shown in Fig. 3 in where  $C_{in}$  and  $C_{out}$  were 248.3 m/s and 268.58 m/s. In addition, A and B were  $90^\circ$  whereas K1 and K2 were determined to be  $90^\circ$  and  $68.46^\circ$ , respectively (see Fig. 3 (a)).

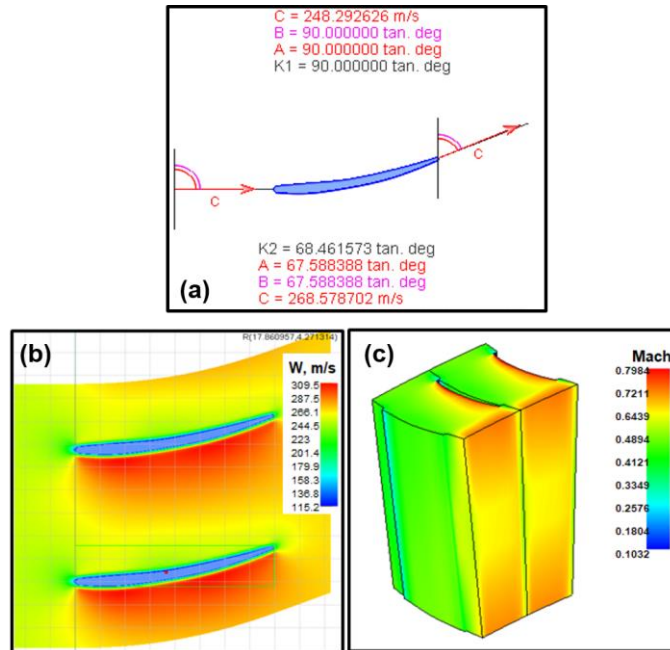


**Figure 3.** (a) absolute velocity and angles of the IGV, (b) relative velocity change at IGVs, (c) Mach number change of flow at IGVs.

A significant relative velocity increase was observed at the pressure sides of the IGVs due to the separation of the airflow from the blade surface (see Fig. 3(b)). Meanwhile, the exit IGV average Mach number was determined to be 0.72 which was in the range of 0.7-1.1 for aerospace application gas turbines [14]. However, the increase in the relative velocity due to the flow separation also increased the Mach number to 0.79 (see Fig. 3(c)).

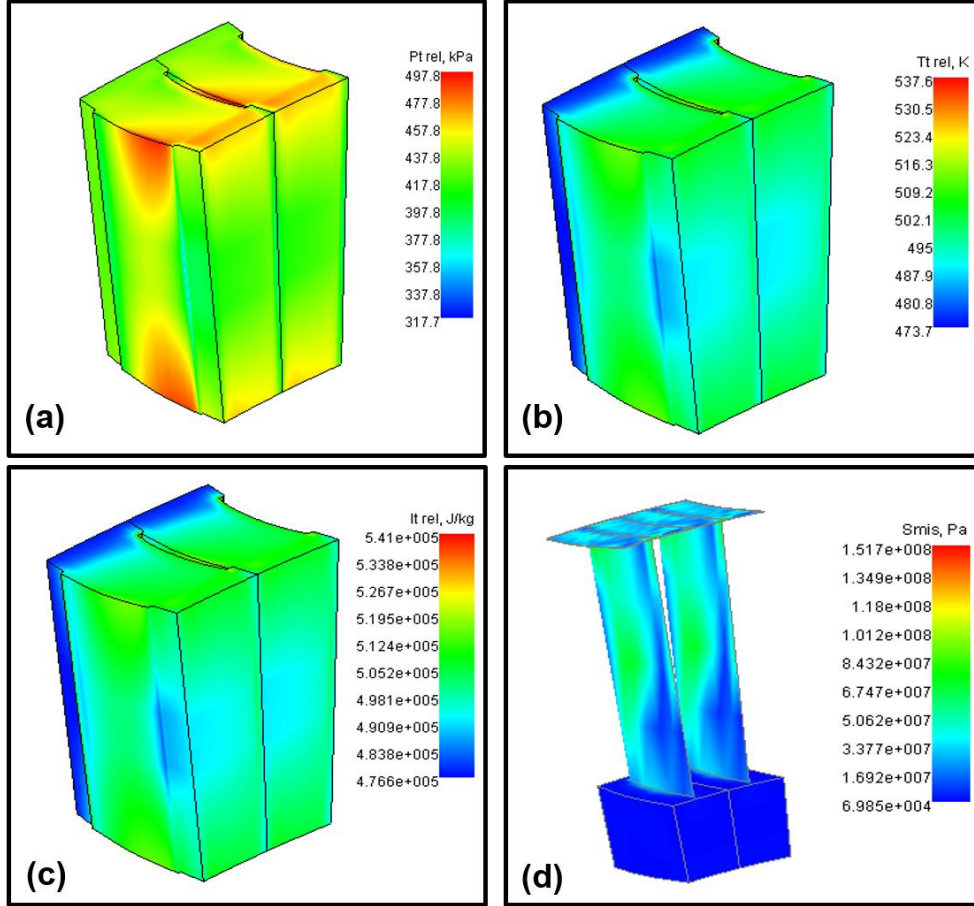


**Figure 4.** CFD analysis of the IGV flow, (a) total pressure, (b) total temperature, (c) total enthalpy change, (d) stress analysis of IGV blade.

The calculated average total pressure of 423 kPa was close to the design inlet pressure of the flow whereas, red areas in the flow indicate the highest total pressure of 461.5 kPa (see Fig. 4(a)). Furthermore, the highest total temperature was calculated to be 503 K while the average temperature was 487 K (see Fig. 4(b)). On the other hand, the average total enthalpy increased from 476.6 kJ/kg to 506.3 kJ/kg (see Fig. 4(b)). Moreover,

according to the Von Mises stress analysis, the maximum calculated stress was 97.12 MPa (see Fig.4(c)).

### **3.2.2. First Stage Analysis**

Fig. 5 shows the first stage velocity triangles where the inlet absolute velocity ( $C$ ) increased from 268.58 m/s to 387.64 m/s at the exit. Meanwhile, inlet rotor relative velocity ( $W$ ) decreased from 458.86 m/s to 332.14 m/s at the exit whereas angular velocity ( $U$ ) was 500.12 m/s and 518.30 m/s at the inlet and exit, respectively. Contrary to rotor blades, stator blades decrease the  $C$  and  $A$  increases at the exit of the stator blade. CFD analysis of the first stage rotor blades was shown in Fig. 6. Relative velocity ( $W$ ) decreased at the inlet from 346 m/s to 262 m/s at the exit with flow separation at the inlet of the blades (see Fig. 6(a)). The total enthalpy of the air was around 668 kJ/kg and did not change significantly at the rotor blades (see Fig. 6(b)). The total temperature and a pressure change of the flow showed the constant average temperature, which was determined to be 635 K that was increased with the total pressure from inlet to exit. The maximum pressure was detected to be 1815 kPa where this pressure was observed left pressure side of the rotor blades at the flow with the average Mach number of 1.09 (see Fig.6(c), (d) and (e)). Stress analysis results in Fig. 6(f) showed that the maximum stress observed near the blade roots with 462 MPa at the first stage of the rotor.

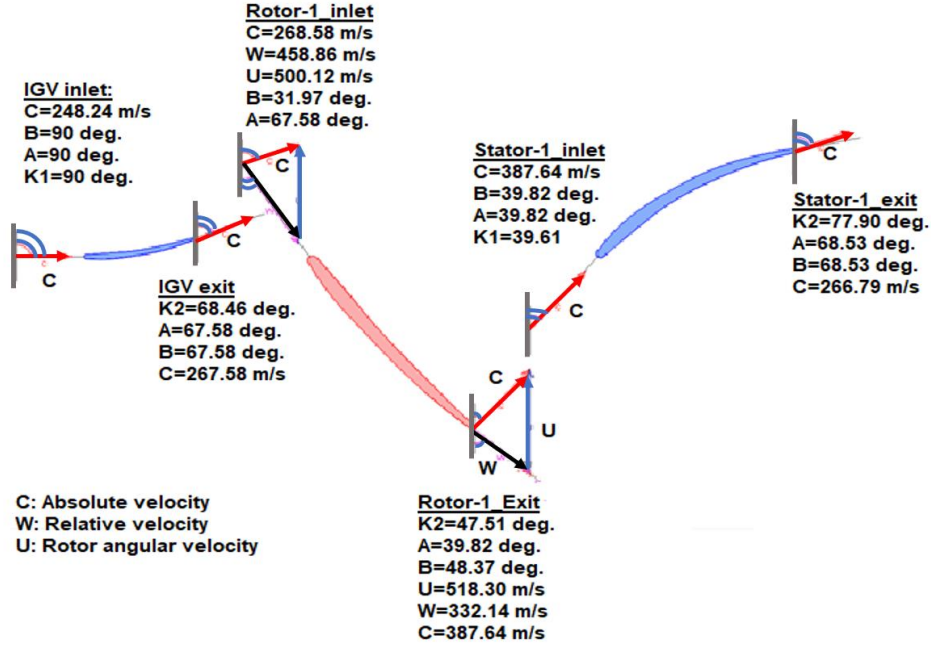


**Figure 5.** Velocity vectors of the first stage with rotor and stator inlet and exit analysis.

When looking at the velocity calculation results of the stator blades, inlet  $C$  was  $387.64$  m/s and angles were determined to be  $K1=39.61^\circ$  whereas  $A$  and  $B$  were  $39.82^\circ$  (see Fig. 5). This velocity and angles changed to  $C=266.78$  m/s,  $K=68.53^\circ$ ,  $B=68.53^\circ$ ,  $A=77.90^\circ$  at the exit of the stator blades. Stator blades decreased the absolute velocity to the inlet of rotor blades at the exit that provided almost constant absolute velocity at the stage. Thermodynamics and stress analysis of the stator blades are shown in Fig. 7. The relative velocity of the flow decreased from  $440$  m/s to  $272$  m/s which was close to  $C$  exit value at the rotor (see Fig. 7(a)). The average total pressure and the temperatures were  $942$  kPa and  $616$  K at the stator blades exit, respectively (see Fig. 7(b), (d)). The total enthalpy changed from  $578.7$  kJ/kg to  $607.2$  kJ/kg at the stator related to absolute velocity decrease at the inlet and exit of the stator (see Eq. 1 and Fig. 7(c)).

*Design and Analysis of an Axial Compressor for a Turbofan Engine*

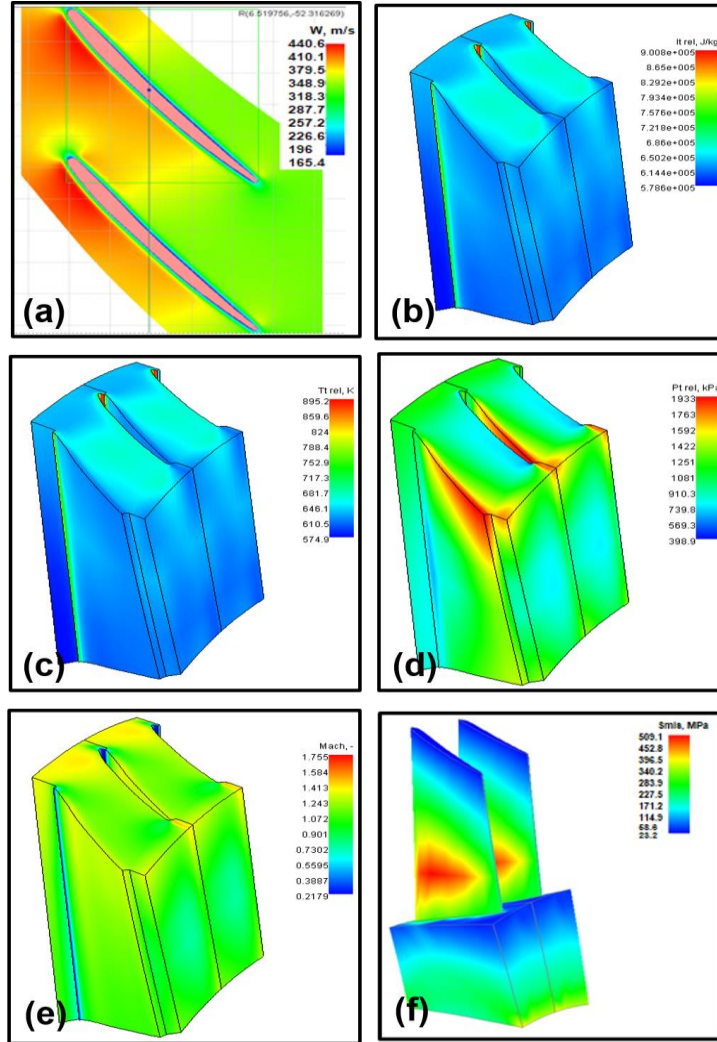


**Figure 6.** First stage rotor thermodynamic and stress analysis, (a) relative velocity of the flow, (b) total enthalpy change of the flow, (c) total temperature change, (d) total pressure change, (e), Mach analysis, (f) stress analysis of the blades.

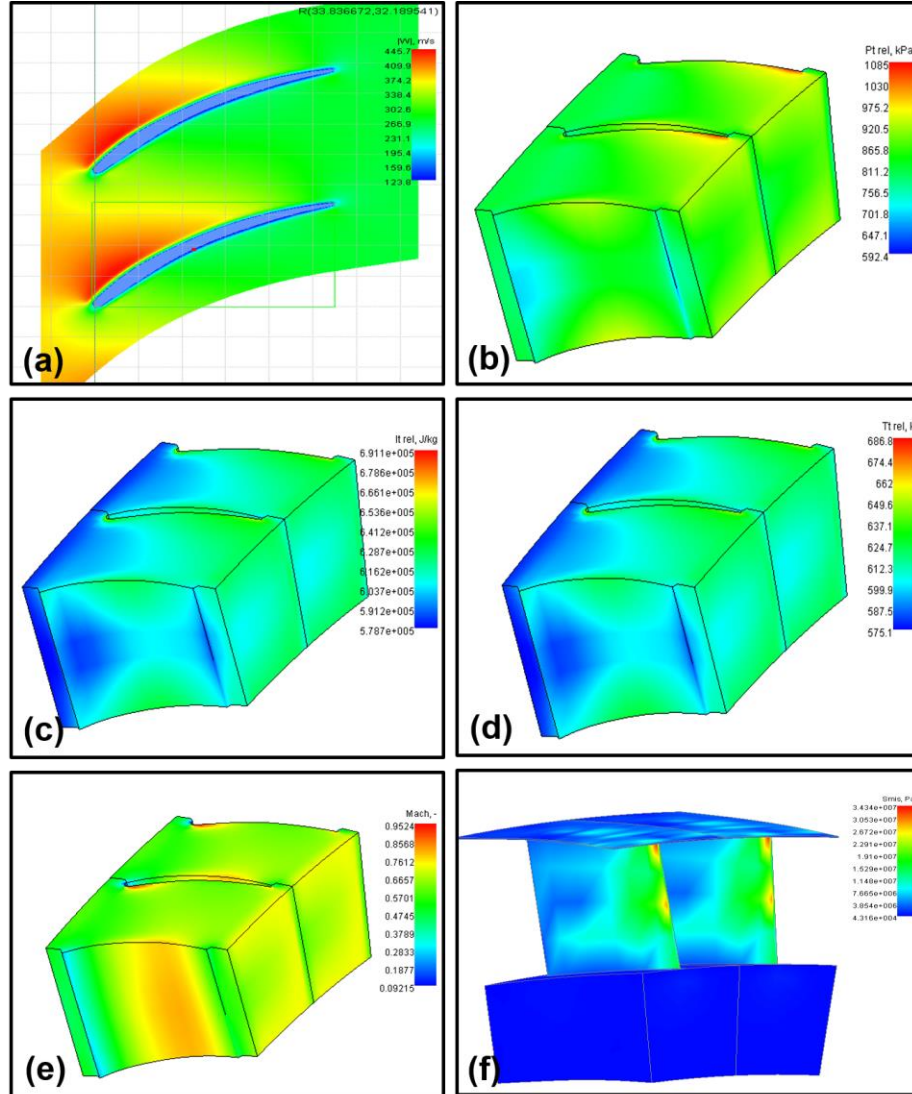


**Figure 7.** First stage stator thermodynamic and stress analysis, (a) relative velocity of the flow, (b) total enthalpy change of the flow, (c) total temperature change, (d) total pressure change, (e), Mach analysis, (f) stress analysis of the blades.

Stator bladed decreased significantly the Mach number which decreased from 1.09 to 0.74 at the exit of stator blades (see Fig. 7(e)). The stress was high at the exit sides of the blades with 30.5 MPa which is very low when compared to rotor blades (see Fig. 7(f)).

### **3.2.3. Fifth Stage Analysis**

Fig. 8 shows the velocity diagram of the last stage consisted of the rotor and stator blades of the axial compressor. The inlet and exit absolute velocity of the stage was 265 m/s. Therefore, the absolute velocity of the air at the combustion chambers was 265 m/s.  $K1$  and  $K2$  were changed from  $23.22^\circ$  to  $49.93^\circ$ ,  $41.81^\circ$  to  $81.45^\circ$  at the inlet and exit of the last stage. CFD analysis of the last stage of the axial compressor is shown in Fig. 9. According to the results, the relative velocity of the air (546 m/s) at the inlet of the stage dropped to 264.38 m/s at the exit. Furthermore, the total pressure of the air at stage exit was found to be 2651 kPa which was close to the design criteria of 2643 kPa (see Fig. 9 (c) and (d)). The total temperature changed from 932 K to 857 K with the total enthalpy change from 942 to 857 kJ/kg at the inlet and exit of the stage that shows total inlet temperature and enthalpy of the air at the inlet of combustion chambers (see Fig. 9 (e) and (f)).

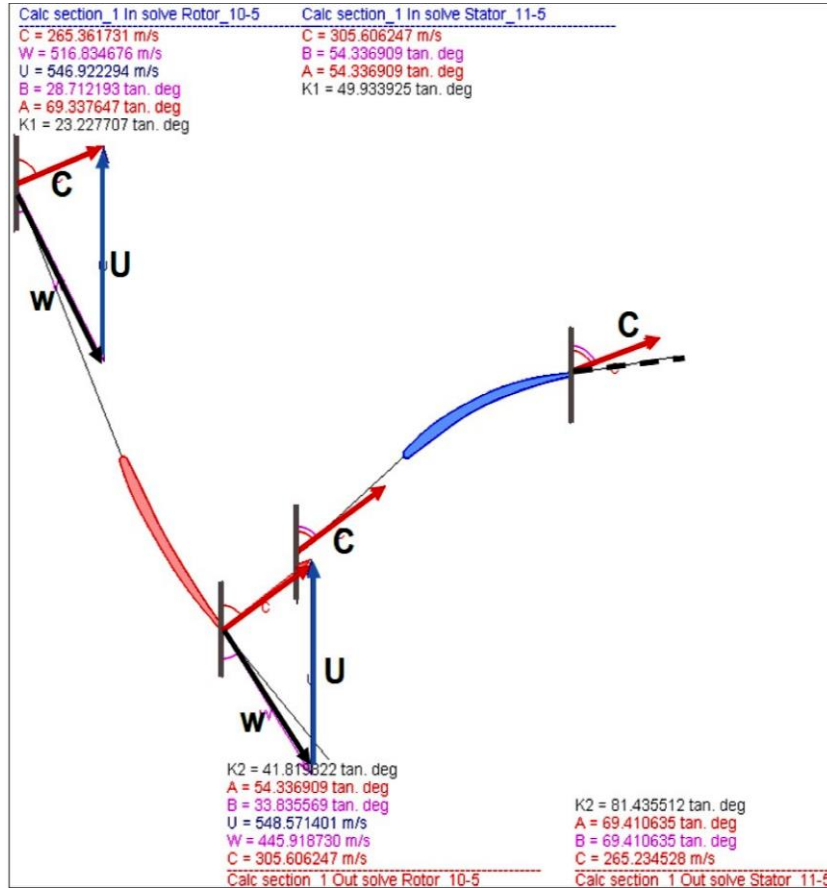


**Figure 8.** Velocity diagram of the last stage of the axial compressor.

The Mach number decreased from 0.95 to 0.49 at the exit of the stage (see Fig. 10 (c) and (d)). The maximum stress of the rotor blades was 365 MPa whereas this stress was determined to be 82 MPa for stator blades (see Fig. 10 (a) and (b)).

*Design and Analysis of an Axial Compressor for a Turbofan Engine*

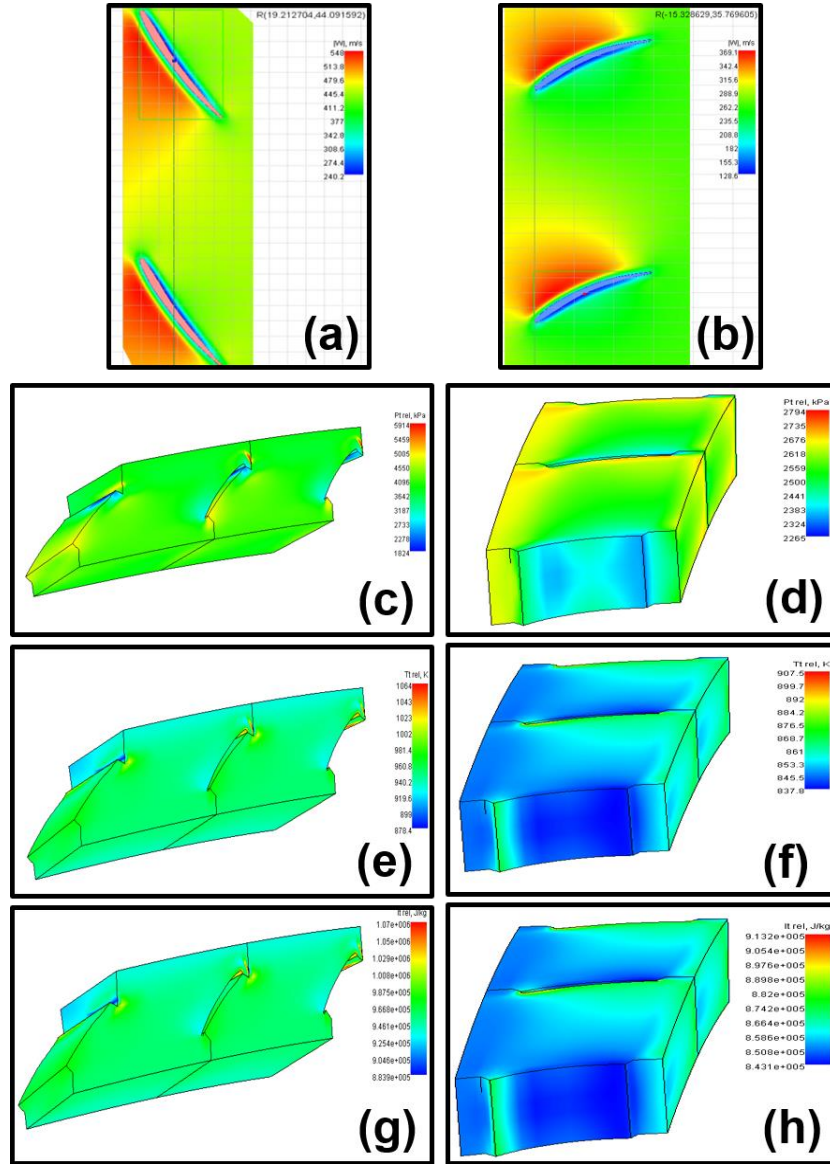


**Figure 9.** Flow analysis of the last stage, (a), (b) relative velocity of the flow at rotor and stator blades, (c), (d) total temperature change of the flow, (e), (f) total temperature change, (g), (h) total enthalpy change of the flow at rotor and stator blades.

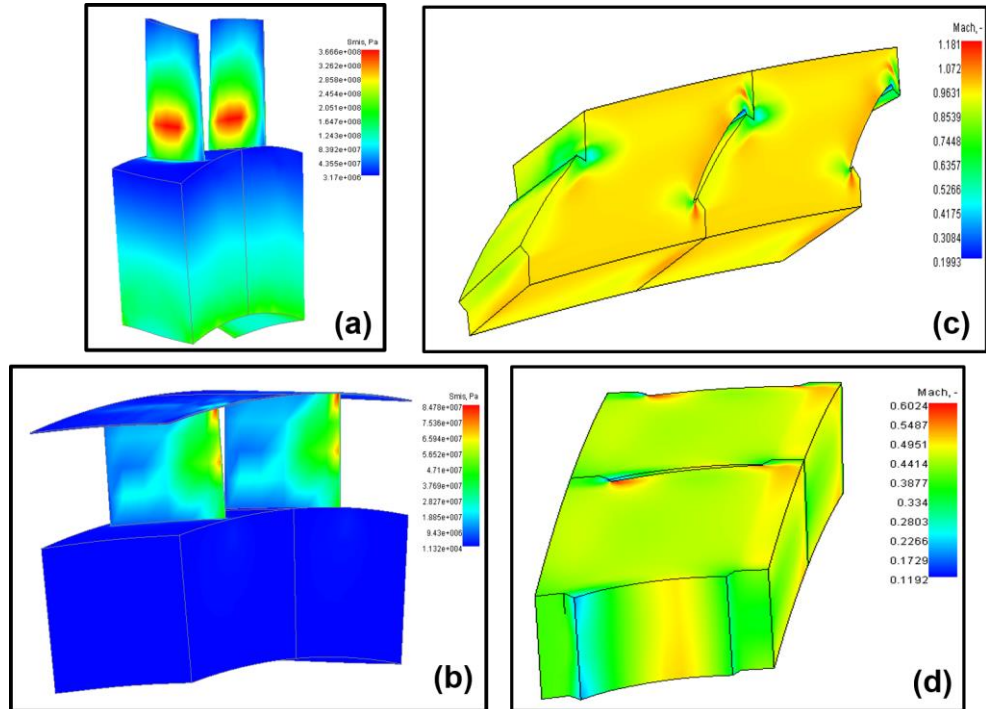


**Figure 10.** (a), (b) stress analysis of the rotor and stator blades, (c), (d) Mach number analysis of the flow at rotor and stator blades.

#### **4. DISCUSSION**

In this study, an axial compressor consisted of 5 stages was designed and analyzed by using AxStream software for a turbofan engine. The design of the compressor was compared to an actual turbofan engine compressor which is used in military aviation. Our design exit temperature at IGV was 487 K which was closed to the actual IVG exit temperature of 475 K. Meanwhile, the last stage temperature was found to be 857 K and this also similar to the actual compressor exit temperature of 833 K. On the other hand, the calculated exit pressure of the designed compressor was 2651 kPa whereas actual compressor pressure was determined to be 2643 kPa.

The results showed that exit temperatures and pressures of the designed compressor were 97% close to the actual compressor. The calculated polyprotic efficiency of the designed compressor was 90% which is higher than reported actual compressor efficiency of 88 %. Nickel-chromium alloy X UNS 06002 was selected as compressor blade material consisted of 8.5 Mo, 21 Cr, 18 Fe, 0.6 W (% in weight). The maximum working temperature and tensile stress of the material blade are 1200 °C and 572.74 MPa. The calculated maximum stress of first and the last stage rotor blades were 462, 365 MPa which are in the safe working limits. On the other hand, the compressor exit temperature of 857 K was lower than the maximum temperature of the blade material. The contribution of the rotor to the increase in pressure is expressed by the reaction rate by rate of rotor and stator pressure differences. Here, the calculated reaction rate was 0.47 close to 50 % that set out the symmetric stage means static pressure increase in stage formed by an equivalent contribution of the rotor and stator. Furthermore, aimed pressure can be achieved with a lower stage by using the symmetric stage and it minimizes the surge and stall in the compressor [15].

## **5. CONCLUSION**

An axial compressor was designed and analyzed with AxStream software for a turbofan engine which is used in military aviation. Five stages of axial compressor velocity, thermodynamics, stress, and CFD analysis were performed. According to this basic analysis, the following conclusion can be drawn:

- Although, rotor blades increased the absolute velocity at the exit stator blades decreased absolute velocity to the inlet of the rotor at the stage. This shows that pressure increase was evaluated at constant absolute velocity.
- CFD analysis of the airflow in the designed compressor showed similar pressure, temperature, and total efficiency with an actual compressor.
- The polyprotic efficiency of the designed compressor was 2 % higher than the actual compressor.
- AxStream is a powerful software for design and analysis of gas turbines main components such as axial compressor, fan, and turbine.

## **REFERENCES**

- [1] Bathie, W.W., (1996). *Fundamentals Of Gas Turbines*, Second Edition, John Wiley&Sons Inc., Canada.
- [2] Eyüp, Ö., (1997). *Türbin Motorlarının Aerotermodinamiği ve Mekaniki Esaslar ve Uygulamalar*, Birsen Yayın Evi, İstanbul.
- [3] Fletcher, P. Philip, W.P., (2004). *Gaz Turbine Performance*, Second Edition, Blackwell Publishing company, Malden, MA, USA.
- [4] Giampaolo, T., (2006). *Gas Turbine Handbook: Principles and Practices*, Third Edition, The Fairmont Press., USA.
- [5] Arthur, G.J., (1994). *Turbine Design and Application*, NASA Scientific and Technical Informantion Program, Washington D.C., USA.
- [6] Rama, G.S.R., Aijaz, K.A., (2003). *Turbomachinery Design and Theory*, Marcel Dekker Inc., USA.
- [7] Theodoro, G., (2001). *Compressor Performance: Aerodynamics For The User*, Second Edition, Elsevier Science & Technology Books, U.S.A.
- [8] Dorfner, C., Hergt, A., Nicke, E., & Moenig, R. (2011). *Advanced Nonaxisymmetric Endwall Contouring for Axial Compressors by Generating an Aerodynamic Separator—Part I: Principal Cascade Design and Compressor Application*. *Journal of Turbomachinery*, 133(2), 021026.
- [9] Richard, H.T.C., (1981). *Gas Turbine Engineering Applications, Cycles and Characteristics*, The Macmillan Press LTD., London/United Kingdom.
- [10] Horlock J.H. (2003). *Advanced Gas Turbine Cycles*, Elsevier Science LTD., Oxford, United Kingdom.

- [11] Samad, A., Kim, K.-Y. (2008). Shape optimization of an axial compressor blade by multi-objective genetic algorithm. Proceedings of the Institution of Mechanical Engineers, Part A: Journal of Power and Energy, 222(6), 599–611.
- [12] Yamada, K., Furukawa, M., Nakakido, S., Matsuoka, A., & Nakayama, K. (2015). Large-Scale DES Analysis of Unsteady Flow Field in a Multi-Stage Axial Flow Compressor at Off-Design Condition Using K Computer. Volume 2C: Turbomachinery.
- [13] Moroz, L., Govorushchenko, Y., Pagur, P. (2006). A Uniform Approach to Conceptual Design of Axial Turbine / Compressor Flow Path, 3rd International Conference, The Future of Gas Turbine Technology, 1-11.
- [14] Boyce, M.P., (2006). Gas Turbine Engineering Handbook, Third Edition, Oxford, UK.
- [15] Ikeguchi, T., Matsuoka, A., Sakai, Y., Sakano, Y., & Yoshiura, K. (2012). Design and Development of a 14-Stage Axial Compressor for Industrial Gas Turbine. Volume 8: Turbomachinery, Parts A, B, and C.